



Scaling and precursor motifs in earthquake networks

Marco Baiesi^{a,b,1}

^a*INFM, Dipartimento di Fisica, Università di Padova, I-35131 Padova, Italy*

^b*Sezione INFN, Università di Padova, I-35131 Padova, Italy*

Received 14 November 2004; received in revised form 25 April 2005

Available online 5 July 2005

Abstract

A measure of the correlation between two earthquakes is used to link events to their aftershocks, generating a growing network structure. In this framework one can quantify whether an aftershock is close or far, from main shocks of all magnitudes. We find that simple network motifs involving links to far aftershocks appear frequently before the three biggest earthquakes of the last 16 years in Southern California. Hence, networks could be useful to detect symptoms typically preceding major events.

© 2005 Elsevier B.V. All rights reserved.

Keywords: Earthquake correlations; Networks; Earthquake prediction

A fundamental open issue in the field of seismicity is whether earthquakes are to some extent predictable or not [1]. There are conflicting points of view about this [1,2]. Nevertheless, phenomenological approaches have been used for some decades to formulate algorithms for earthquake prediction [3–6], sometimes based on the search for complex (long-range) correlations [3].

Insight into the issue of seismicity and maybe of earthquake prediction can be obtained by measuring the correlations between any pair of earthquakes. One method to estimate the amount of correlation was put forward in Ref. [7] (see also

E-mail address: baiesi@pd.infn.it.

¹Present address: Instituut voor Theoretische Fysica, K.U.Leuven 3000, Belgium.

Ref. [8]), based on the statistical properties of earthquakes. If epicenters are distributed with a fractal dimension d_f , the mean number of events within an area of radius l should scale as l^{d_f} . According to the Gutenberg–Richter law [1], the number of these events with magnitude $\geq m$ is proportional to 10^{-bm} , with $b \approx 1$. Of course, the number of these events is on average also proportional to the time t we have been spending to record them. Hence, globally the mean number of events scales with the size of the space-time-magnitude window as $n \simeq K t 10^{-bm} l^{d_f}$, where K is a constant related to the seismic activity. When a new event j takes place, it defines a point of view from which one can assess whether past seismic events appear unusual or usual, with respect to their expected average number. Indeed, any pair of events (i, j) , separated by a time interval t_{ij} and a distance l_{ij} , defines an expected number of events $n_{ij} = K t_{ij} 10^{-bm_i} l_{ij}^{d_f}$, where m_i is the magnitude of the first event.

One finds small n_{ij} values when j occurs immediately after i , very close to i , and if i has a large magnitude. A very small n_{ij} value means that an event with magnitude m_i had very small probability to occur in the space-time window defined by event j . Since such a case should rarely take place at random, its actual occurrence tells us that i and j are correlated. Furthermore, the smaller is n_{ij} , the more unusual is event i “with respect to j ”, the more i and j are correlated,¹ as it was argued in Ref. [7]. Hence, one can adopt n_{ij} as a metric for quantifying correlations between events. On the basis of n_{ij} one can also build a network of earthquakes [7] by drawing an oriented link to a new event j only from the event i giving the smallest n_{ij} value (denoted as n_j^*). In this pair, we call event i the “main shock” and j is the “aftershock” even if $m_j > m_i$.²

In this paper we examine such earthquake correlation graphs by means of tools of network theory. We show that the notion of distance at the basis of the network construction underlies remarkable statistical scaling properties, which should reflect basic mechanisms of earthquake formation and propagation. We also find that some simple motifs (small pieces composed by a few nodes and links [9]) could constitute an interesting kind of precursor of major events. The study of the motif occurrences is a strategy to understand the properties of the systems described by networks [9]. For example, it is currently believed that understanding the statistics of simple motifs in protein–protein interactions and transcription regulatory networks can help to understand the metabolism [9–13].

The catalog we have analyzed is maintained by the Southern California (SC) Earthquake Data Center [14]. Data in the period ranging from the 1st of January 1984 to the 31st of December 2003, and earthquakes with magnitude $m \geq m_c = 3.0$ are considered (8858 events). In the area covered by the catalog the Gutenberg–Richter law holds with $b \simeq 0.95$ [15], and $d_f = 1.6$ [16]. Quantities are always measured in MKS units.

We examine the three-dimensional distribution of earthquakes, taking into account their epicenters (latitude and longitude) and depths, i.e., their hypocenters.

¹This way of thinking is rather general and can be applied to contexts different from seismicity as well.

²As discussed in Ref. [7], the standard aftershock collection instead would count all events following a stronger earthquake, in a given time window and far less than a maximum distance.

The spatial separation between events is given by the Euclidean distance between their hypocenters, and the fractal dimension of hypocenters is supposed to be $D_f = 1 + d_f = 2.6$. The metric we use is then

$$n_{ij} = K' l_{ij}^{D_f} 10^{-b m_i} t_{ij} .$$

With this metric a network will be constructed by the following two simple rules:

- R1: Keep only links that denote strong correlations.
- R2: For each node, keep the incoming link that brings the strongest correlation and a few ones that are nearly as important as that one.

Links reliably denoting correlations have $n_{ij} \leq n_c$, with a suitable threshold n_c^3 [7]. In order to define a selection procedure independent of the constant K' , here we use $n_c = \langle n^* \rangle / 10$, where $\langle n^* \rangle$ denotes the average of all n_i^* with $i = 2, 3, \dots, j - 1$.

If at most one incoming link per node is allowed, the network has the form of a growing tree [7]. We relax this constraint because we want a richer network structure, with abundance of motifs like triangles of linked nodes, which are usually associated with the presence of non-trivial correlations within networks [17–19]. Nearly optimal incoming links to a new event have n_{ij} slightly greater than their minimum value n_j^* and are the first candidates to be added to the tree structure: hence, we choose to draw a link when $n_{ij} \leq n_c$ (R1) and $n_{ij} \leq \phi n_j^*$ (R2), with constant $\phi > 1$ (this procedure is also suggested by the fact that data from catalogs have experimental errors). We set $\phi = 10$, obtaining roughly two incoming links per node, but other similar values do not considerably alter the results. This is one among several ways of building general earthquake networks, see for instance another example in Ref. [8].

Our analysis of the precursory phenomena is based on the statistics of the quantity

$$\rho_{ij} = l_{ij}^{D_f} 10^{-b m_i} ,$$

which is the space-magnitude part of the metric values n_{ij} associated with drawn links. In Fig. 1 we show its distribution $P(\rho)$. In addition, we also plot the distributions of ρ relative to links departing from shocks in ranges of magnitudes $[m_1, m_2)$, denoted as $P_{[m_1, m_2)}(\rho)$. Two distinct power laws appear in $P(\rho)$ as well as in all $P_{[m_1, m_2)}(\rho)$ considered. For $\rho \rightarrow 0$, $P(\rho) \sim \rho^{-\alpha}$, with $\alpha \simeq 0.3$. In the regime $\rho \rightarrow \infty$ instead $P(\rho) \sim \rho^{-\beta}$, with $\beta \simeq 1.55$. Since all $P_{[m_1, m_2)}(\rho)$ are quite well overlapped, and the aftershock distances vary weakly with time after an event (not shown), a length $l_m = \rho^{1/D_f} = 10^{(b/D_f)m}$ is a good unit for measuring the distance of aftershocks from an event of magnitude m . Thus, the exponent $\sigma = b/D_f \simeq 0.37$ might justify the rescaling of aftershocks distances with a factor $10^{\sigma m}$, as it was done in Ref. [7] ($\sigma \simeq 0.4$ there).

The distributions $P(\rho)$ describes a property of individual correlations between pairs of earthquakes, from which we clearly see that two classes of aftershocks exist,

³In order to avoid infinite spatial windows for $t \rightarrow 0$, a minimum time interval $t_{\min} = 60$ s between two events is imposed. The precise value of t_{\min} is not important, as only a few links over thousands change if we choose a different t_{\min} . In the metric, a minimum distance $l_{\min} = 100$ m is also used.

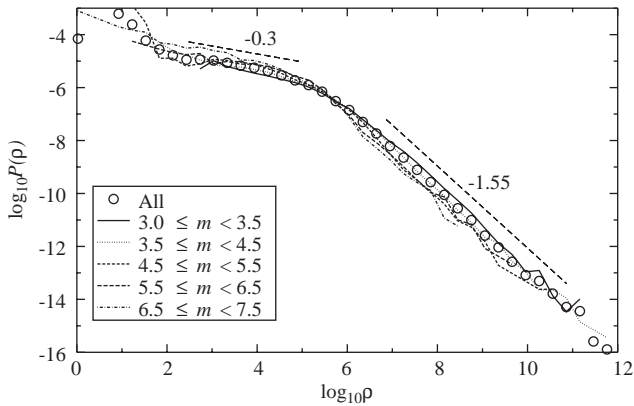


Fig. 1. Log–log plot of the global distribution $P(\rho)$ (circles), and of the distributions $P_{[m_1, m_2]}(\rho)$ generated by earthquakes with magnitude in ranges $[m_1, m_2)$ (see legend). Two power-law regimes (with relative exponents) are evidenced by dashed straight lines.

corresponding to the two regimes of $P(\rho)$. A geophysical explanation of these two regimes could be related to the hierarchical fault structure: possibly, small ρ are connected to the conventional aftershocks within the rupture area, while the high ρ region could be determined mainly by inter-fault aftershocks, which are also detected by our method.

A wide area of aftershock activity, as quantified by a large ρ value, may be favored by high stresses within the crust, and hence may be related to the periods prior to strong earthquakes. During these periods, it is also reasonable to find complex correlations in the stress field [20]. We have tested the possibility that these phenomena are highlighted by peculiar network motifs, i.e., by studying the local topological structure of the growing network of earthquakes. Indications supporting our hypothesis can be found by modifying the notion of local clustering coefficient of a node, which is normally given by the fraction of triangles it forms with its neighbors [17–19]. In order to meet our former requirements, the motifs we study here are special triangles (ST), in which the ρ value carried by the first link (i – k link in the inset of Fig. 2) is larger than a given threshold ρ_0 . The special clustering coefficient of a new node j is then $C_j = \Delta_j / \Delta_j^{\max}$, where Δ_j is the number of ST it forms with its κ_j main shocks, and $\Delta_j^{\max} = \kappa_j(\kappa_j - 1)/2$. By definition $C_j = 0$ if $\kappa < 2$.

To show that ST may be precursors of strong events we proceed as follows: the first 3 years of the catalog are used to obtain an initial estimate of $\langle n^* \rangle$. During the next year we just add links, to avoid possible problems arising from the analysis of a network where links to old events are lacking. Then, from the beginning of 1988, an algorithm analyzes the signal given by the C value, evaluated for each event when it takes place. When $C > 0$, we start an integration of the C signal, called C_I , which is reset to zero if $C = 0$ for a period T_0 . Values $T_0 = 60$ days and $\rho_0 = 10^7$ yield a reasonable overall rate of $C > 0$ values (spikes $0 < C \leq 1$ in Fig. 2), avoiding the saturation of C_I , which is the signal that we think is somewhat proportional to the

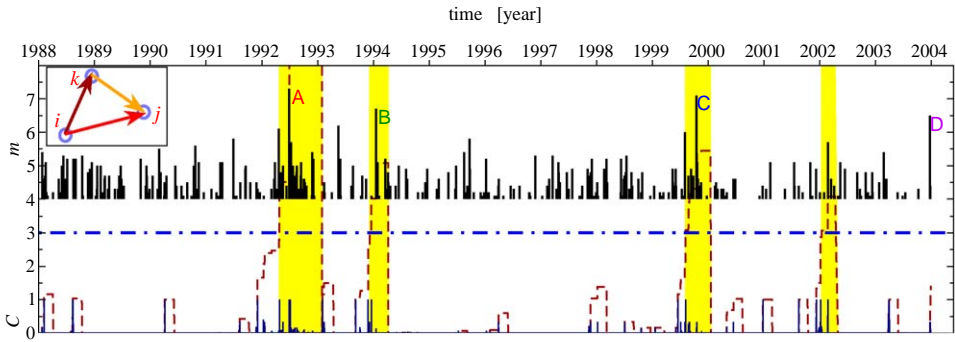


Fig. 2. Time series of event magnitudes (above, only $m \geq 4$ are shown) and of special clustering C of events (below). Landers (A), Northridge (B), Hector Mine (C), and San Simeon (D) are the four biggest events since 1988 in the catalog. The integrated signal C_I is shown as a dashed line, while the horizontal dot-dashed line represents the threshold value $C_H = 3$; when $C_I > C_H$, alarms are declared (shaded areas). Inset: sketch of a triangle of linked events, which is “special” if $\rho_{ik} > \rho_0$.

seismic hazard in the region. The periods when C_I is greater than a constant threshold $C_H = 3$ are declared as alarms.

Fig. 2 suggests that there is a relation between alarm times and the occurrence of the three biggest events in the catalog: for Landers event [$m = 7.3$, labeled with (A)], alarm would have started 9 weeks before its occurrence, for Northridge [(B), $m = 6.7$] one had to wait 6 weeks after the declaration of the alarm, while the alarm before Hector Mine [(C), $m = 7.1$] started 10 weeks in advance. Thus, they would have been predicted in the short term. The San Simeon event [(D), $m = 6.5$] instead was not within an alarm time, while an alarm was also declared in a period when the biggest event had $m = 5.7$.

The spatial location of the precursor motifs is another interesting issue. Figs. 3 and 4 show the distribution of ST giving rise to the alarms (i.e., when $C_I > 0$) before the three biggest events. In Fig. 3, small letters corresponding to the big event ones denote areas with ST, and three insets show enlargements of some of them. Excluding a cluster of ST which would have indicated the future location of Landers epicenter [Fig. 3(i1)], ST do not appear close to the location of the incoming big events, in agreement with the idea that the preparation of an earthquake is not localized around its future source (see Ref. [3] and references therein).

A plausible explanation of both this delocalization of the precursor patterns with respect to the big shock and the relation between high ρ values and strong earthquakes might come from the critical point scenario [20–24], in which a big event represents a finite time singularity [25]. Indeed, as in the theory of critical phenomena, a suitably defined correlation length shows a singular behavior diverging prior to big earthquakes [26,27,5]. This length is evaluated by a procedure which sums the distances between events which are not aftershocks. Due to our results, we believe that aftershock distances may be a complementary indicator of long-range correlations, and in particular that relatively far aftershocks could be a

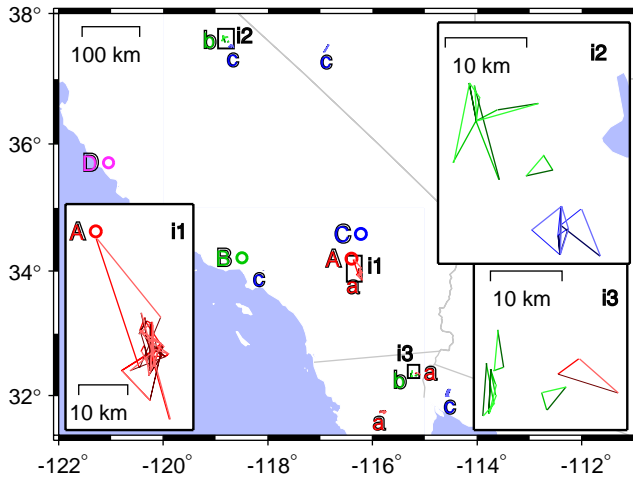


Fig. 3. Location of big events (circles, same capital letters discussed in the text and in Fig. 2), and of precursor patterns (ST), marked with the same letter of the relative big shock. The three insets are enlargements of areas with ST. Color tones of the three links in a triangle follow the same order as in the inset of Fig. 2; in particular the older link is darker.

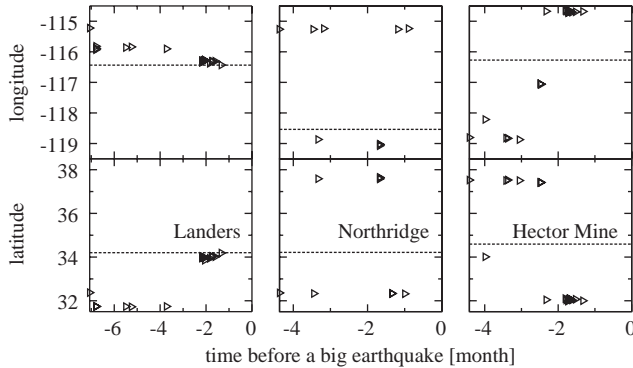


Fig. 4. Longitude and latitude of the last node of ST, during the period when $C_I > 0$ before Landers, Northridge and Hector Mine events. The coordinates of the big events are plotted as dashed lines. There is a clear convergence of the ST to the Landers epicenter [see also Fig. 3(i1)].

typical symptom of an incoming strong earthquake. Notice that we obtain useful information also from the statistics of the aftershocks of the numerous minor earthquakes, in agreement with the idea that the latter are active players in seismicity [28].

To assess the stability of our simple algorithm, in Fig. 5 we have plotted an error diagram [29] where the fraction of events with $m \geq m_>$ that are not predicted is shown as a function of the fraction of alarm time. In the diagram, the performance

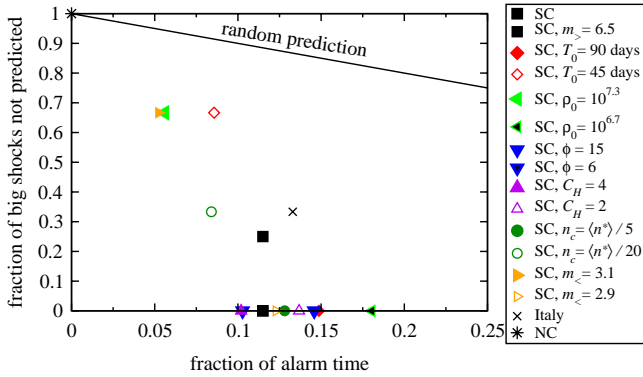


Fig. 5. Error diagram. Symbols are associated with geographic zones and eventually with a modified parameter (see text). The line represents the performance of a random alarm declaration.

of a random alarm declaration is represented by a line joining the point (0, 1) with (1, 0). Starting from the point ($n_c = \langle n^* \rangle / 10$, $\phi = 10$, $\rho_0 = 10^7$, $C_H = 3$, $T_0 = 60$ days, $m_< = 3.0$, $m_> = 6.7$) in the parameter space, we have varied one of the parameters per time, around its initial point, and plotted the relative performance in Fig. 5. One clearly see that the algorithm does better than a random alarm declaration, and that it is reasonably stable.

The case illustrated in this paper confirms that a translation of issues of seismicity into a network problem can be a fruitful approach [7,8,30,31]. In order to have further insight on this possibility, we have analyzed two other catalogs, centered around Northern California (NC) and Italy [32], and covering the same time span of our SC catalog. We have used the same parameters of SC, but for NC we set $m_> = 6.5$ to include both S. Simeon and Loma Prieta (1989, $m = 7$) events in the big shock list. The algorithm does not recognize any of the two NC big events (no alarms declared, see Fig. 5). This reminds us that, at this stage, this algorithm is just a retrospective statistical tool used to support the view that the Earth crust sometimes manifests signs of instability before big earthquakes. However, lowering $m_<$ and using some refinements (see below) it is possible to include both big events in an alarm time [33].

In Italy we set $\rho_0 = 10^8$ and a shift of the magnitudes ($m_< = 2.5$, $m_> = 5.8$) is necessary in order to include the two largest events (Umbria 1997, $m = 6$ and Molise 2002, $m = 5.9$) in the big shock list and a considerable number of smaller ones in the analysis. In this case, $\frac{4}{6}$ of the big events are predicted, including the two most disruptive ones, with a fraction of alarm time ≈ 0.13 , as shown in Fig. 5.

Possible improvements of this approach should take into account the impossibility of precisely assign a hypocenter to each earthquake. This is due to the experimental finite precision as well as to an intrinsic property of earthquakes, which are not exactly pointwise processes. A preliminary investigation, where only sufficiently long links in space with $\rho > \rho_0$ are allowed to give rise to ST, is showing good results in all

cases considered above [33], as well as in Eastern Mediterranean and Southern Japan.

In summary, by means of an appropriate metric quantifying the amount of correlation between earthquakes, aftershocks of any event can be identified. Aftershock distances from a shock of magnitude m are properly measured by a length unit scaling as $10^{0.37m}$. This information has been combined with a study of the local topology of the growing network of earthquakes, to show that simple motifs embodying links to unusually far aftershocks appeared frequently before Landers, Northridge and Hector Mine events in Southern California. This does not mean that we have developed a prediction method yet. Future investigations, for example, should consider more geological areas and verify how often a sequence of special motifs is followed by a big earthquake.

Acknowledgements

The author thanks A. Kabakçioğlu, E. Orlandini, M. Paczuski and A.L. Stella for the useful comments and discussions. It is acknowledged the support from INFM-PAIS02, and the free download of excellent data available in the web sites of SCEDC [14] and NCEDC [32].

References

- [1] C.H. Scholz, *The Mechanics of Earthquakes and Faulting*, second ed., Cambridge University Press, Cambridge, 2002.
- [2] “Is the reliable prediction of individual earthquakes a realistic scientific goal?”, see the web page <http://www.nature.com/nature/debates/index.html>, 1999.
- [3] V. Keilis-Borok, Earthquake prediction: state-of-the-art and emerging possibilities, *Annu. Rev. Earth Planet. Sci.* 30 (2002) 1–33.
- [4] V.I. Keilis-Borok, P.N. Shebalin, I.V. Zaliapin, Premonitory patterns of seismicity months before a large earthquake: five case histories in Southern California, *Proc. Natl. Acad. Sci. USA* 99 (2002) 16562–16567.
- [5] I. Zaliapin, Z. Liu, G. Zöller, V. Keilis-Borok, D. Turcotte, On increase of earthquake correlation length prior to large earthquakes in California, *Comp. Seism.* 33 (2002) 141–161.
- [6] V. Keilis-Borok, P. Shebalin, A. Gabrielov, D. Turcotte, Reverse detection of short-term earthquake precursors, *Phys. Earth Planet. Inter.* 145 (1–4) (2004) 75–85.
- [7] M. Baiesi, M. Paczuski, Scale-free networks of earthquakes and aftershocks, *Phys. Rev. E* 69 (2004) 066106.
- [8] M. Baiesi, M. Paczuski, Complex networks of earthquakes and aftershocks, *Nonlin. Proc. Geophys.* 12 (2005) 1–11.
- [9] R. Milo, et al., Network motifs: simple building blocks of complex networks, *Science* 298 (2002) 824–827.
- [10] E. Ziv, R. Koytcheff, M. Middendorf, C. Wiggins, Systematic identification of statistically significant network measures, *Phys. Rev. E* 71 (2005) 016110.
- [11] S. Wuchty, Z.N. Oltvai, A.L. Barabási, Evolutionary conservation of motif constituents in the yeast protein interaction network, *Nat. Genet.* 35 (2) (2003) 176–179.
- [12] E. Yeger-Lotem, et al., Network motifs in integrated cellular networks of transcription-regulation and protein–protein interaction, *Proc. Natl. Acad. Sci. USA* 101 (16) (2004) 5934–5939.

- [13] M. Middendorff, et al., Discriminative topological features reveal biological network mechanisms, *BMC Bioinformatics* 5 (2004) 181.
- [14] <http://www.data.secc.org/ftp/catalogs/SCSN/>
- [15] P. Bak, K. Christensen, L. Danon, T. Scanlon, Unified scaling law for earthquakes, *Phys. Rev. Lett.* 88 (2002) 178501.
- [16] A. Corral, Local distributions and rate fluctuations in a unified scaling law for earthquakes, *Phys. Rev. E* 68 (2003) 035102(R).
- [17] D.J. Watts, S.H. Strogatz, Collective dynamics of ‘small-world’ networks, *Nature* 393 (6684) (1998) 440–442.
- [18] R. Albert, A.-L. Barabási, Statistical mechanics of complex networks, *Rev. Mod. Phys.* 74 (2002) 47–97.
- [19] S.N. Dorogovtsev, J.F.F. Mendes, Evolution of networks, *Adv. Phys.* 51 (2002) 1079–1187.
- [20] S.C. Jaumé, L.R. Sykes, Evolving towards a critical point: a review of accelerating seismic moment/energy release prior to large and great earthquakes, *Pure Appl. Geophys.* 155 (1999) 279–305.
- [21] L.R. Sykes, S.C. Jaumé, Seismic activity on neighboring faults as a long-term precursor to large earthquakes in the San Francisco bay area, *Nature* 348 (1990) 595–599.
- [22] C.G. Bufe, D.J. Varnes, Predictive modelling of the seismic cycle of the greater San Francisco bay region, *J. Geophys. Res.* 98 (1993) 9871–9883.
- [23] D.D. Bowman, G. Ouillon, C.G. Sammis, A. Sornette, D. Sornette, An observational test of the critical earthquake concept, *J. Geophys. Res.* 103 (1998) 24359–24372.
- [24] D.D. Bowman, G.C.P. King, Accelerating seismicity and stress accumulation before large earthquakes, *Geophys. Res. Lett.* 28 (2001) 4039–4042.
- [25] C.G. Sammis, D. Sornette, Positive feedback, memory, and the predictability of earthquakes, *Proc. Natl. Acad. Sci. USA* 99 (2002) 2501–2508.
- [26] G. Zöller, S. Hainzl, J. Kurths, Observation of growing correlation length as an indicator for critical point behavior prior to large earthquakes, *J. Geophys. Res.* 106 (2001) 2167–2176.
- [27] G. Zöller, S. Hainzl, A systematic spatiotemporal test of the critical point hypothesis for large earthquakes, *Geophys. Res. Lett.* 29 (2002) 53.
- [28] A. Helmstetter, Is earthquake triggering driven by small earthquakes, *Phys. Rev. Lett.* 91 (2003) 058501.
- [29] G.M. Molchan, Earthquake prediction as a decision-making problem, *Pure Appl. Geophys.* 149 (1997) 233–247.
- [30] S. Abe, N. Suzuki, Scale-free network of earthquakes, *Europhys. Lett.* 65 (2004) 581.
- [31] S. Abe, N. Suzuki, Scale-invariant statistics of period in directed earthquake network, *Euro. Phys. J. B* 44 (2005) 115–117.
- [32] <http://quake.geo.berkeley.edu/anss/catalog-search.html>
- [33] M. Baiesi, unpublished.